Supplementary file for:

Weakening of Decadal Variation of Northern Hemisphere Land Monsoon Rainfall under Global Warming

Yeyan Jiang[1], Juan Li[1], Bin Wang[2], Youngmin Yang[1], Zhiwei Zhu[1]

[1]*Key Laboratory of Meteorological Disaster, Ministry of Education (KLME)/Joint International Research Laboratory of Climate and Environment Change (ILCEC)/Collaborative Innovation Center on Forecast and Evaluation of Meteorological Disasters (CIC-FEMD), Nanjing University of Information Science and Technology, Nanjing, 210044, China*

[2]*Department of Atmospheric Sciences and International Pacific Research Center, the University of Hawaii at Manoa, Honolulu HI 96822, USA*

Corresponding author: Zhiwei Zhu (zwz@nuist.edu.cn)

This file includes Supplementary Figures 1–12 and Supplementary Tables 1–4:

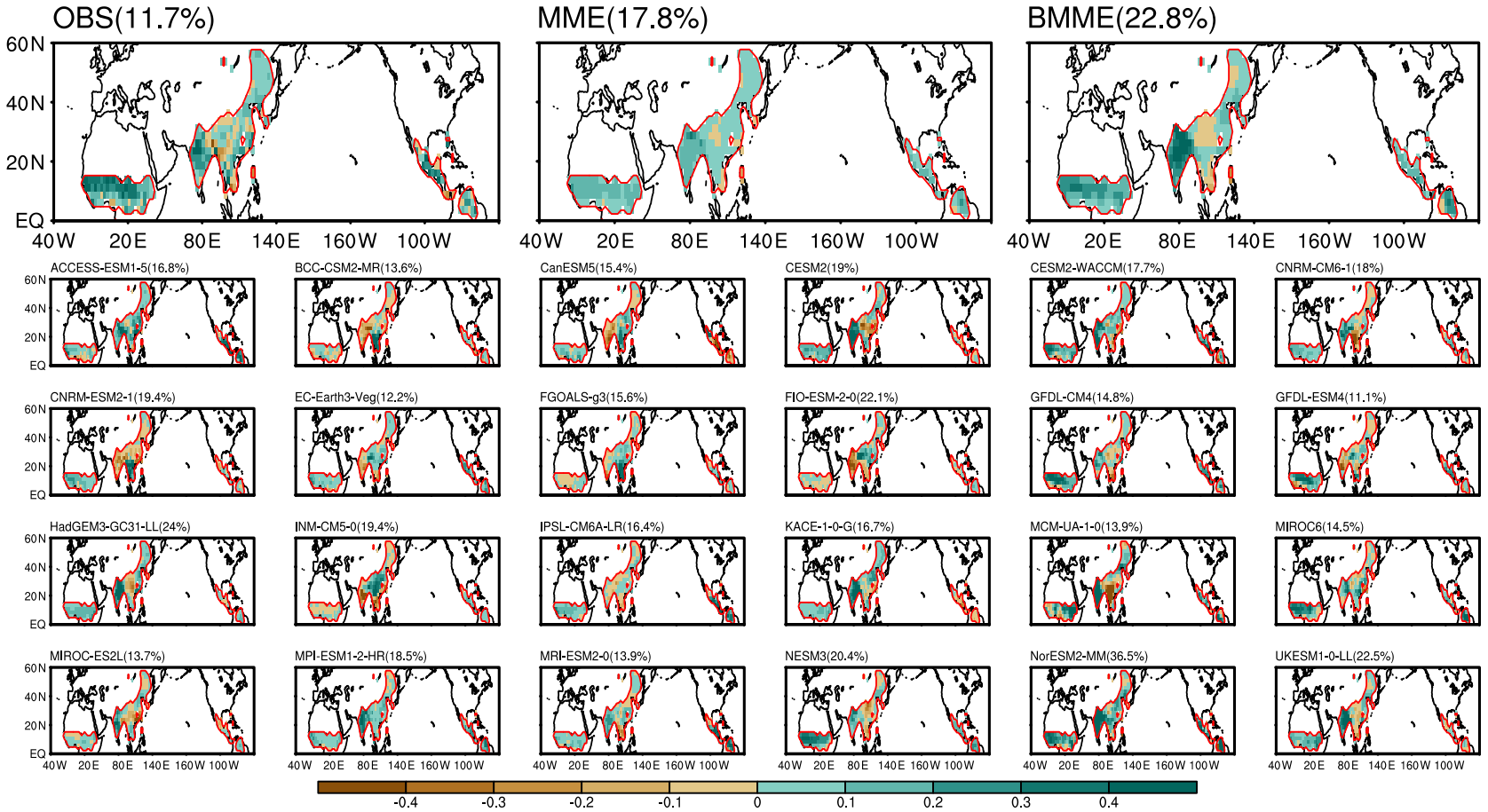

Supplementary Figure 1. The spatial pattern of the first EOF mode of the detrended and 4-yr running mean summer (MJJAS) rainfall during historical period (1901-2014). Spatial patterns of the first EOF mode in observation (OBS), ensemble mean of all models (MME) as well as the best six models (BMME) and individual models in historical run. The number of each single subfigure represents the explained variance of the EOF mode. The result of MME (BMME) is the average of the EOF modes obtained from all CMIP6 models (best six models). The NH land monsoon domains are outlined by the red contours.

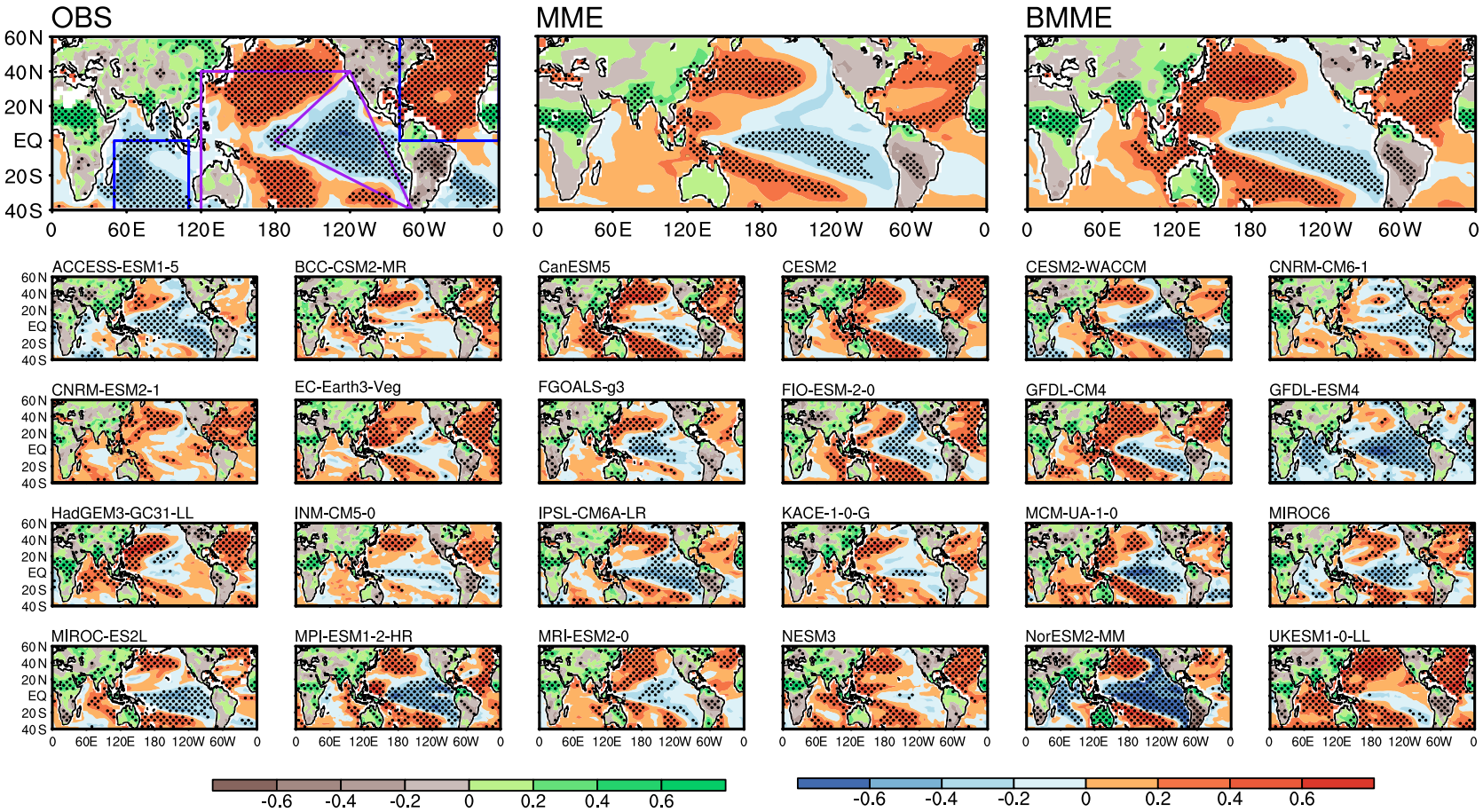

Supplementary Figure 2. SSTAs associated with the decadal NHLMR index during historical period (1901-2014). The correlation maps of boreal summer (MJJAS) SST (shading over the ocean) and land rainfall (shading over the land) with respect to the decadal NHLMR index in observation and historical simulations from MME, BMME and individual models. The result of MME (BMME) is the average of the correlation maps obtained from 24 CMIP6 models (best six models). The correlation coefficients significant at a 95% confidence level by a Monte Carlo test are dotted. The blue and purple lines outline the areas used for defining the NAID and EWPC indexes in observation, respectively.

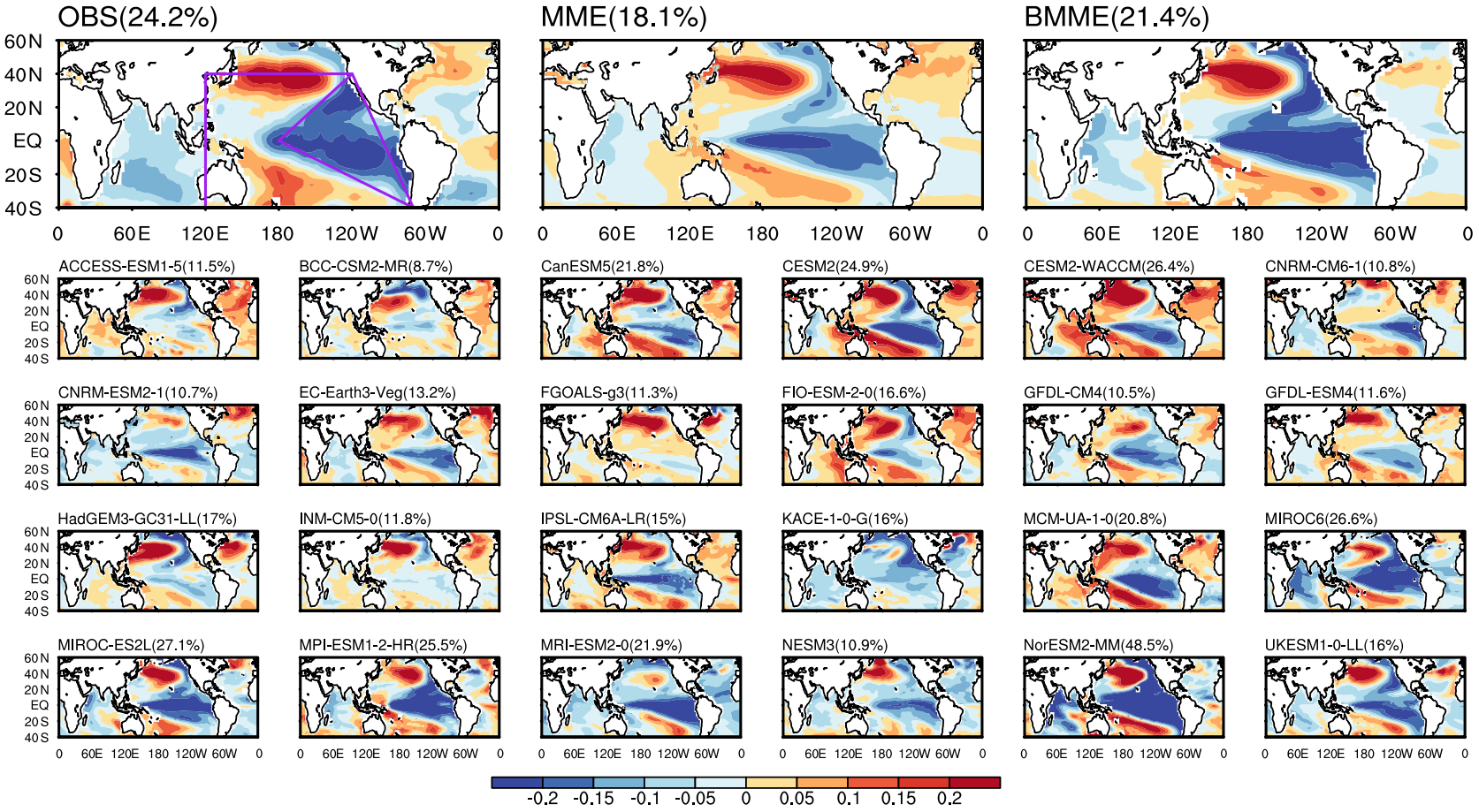

Supplementary Figure 3. The EWPC mode in CMIP6 models' historical simulation and observation during the period of 1901-2014. The EWPC mode of global SST in OBS, MME, BMME and individual models in historical run. The number on left conner of each subfigure represents the explained variance of the EOF mode. The result of MME (BMME) is the average of the EWPC modes obtained from all CMIP6 models (best six models). The EWPC domain is outlined by the purple lines in OBS.

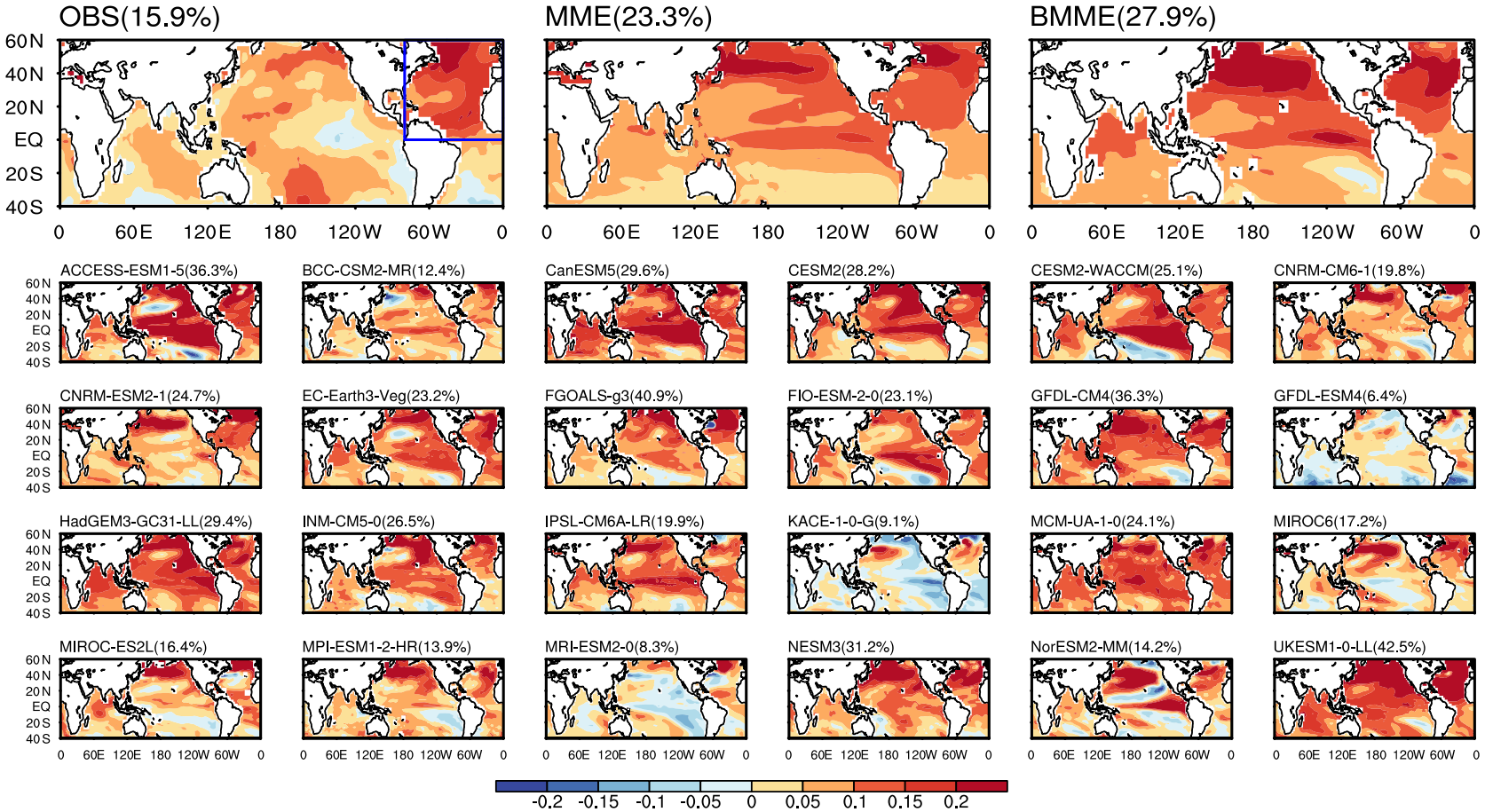

Supplementary Figure 4. The NA mode in CMIP6 models' historical simulation and observation during the period of 1901-2014. The NA mode of global SST in OBS, MME, BMME and individual models in historical run. The number on left conner of each subfigure represents the explained variance of the EOF mode. The result of MME (BMME) is the average of the NA modes obtained from 24 CMIP6 models (best six models). The NA domain is outlined by the blue lines in OBS.

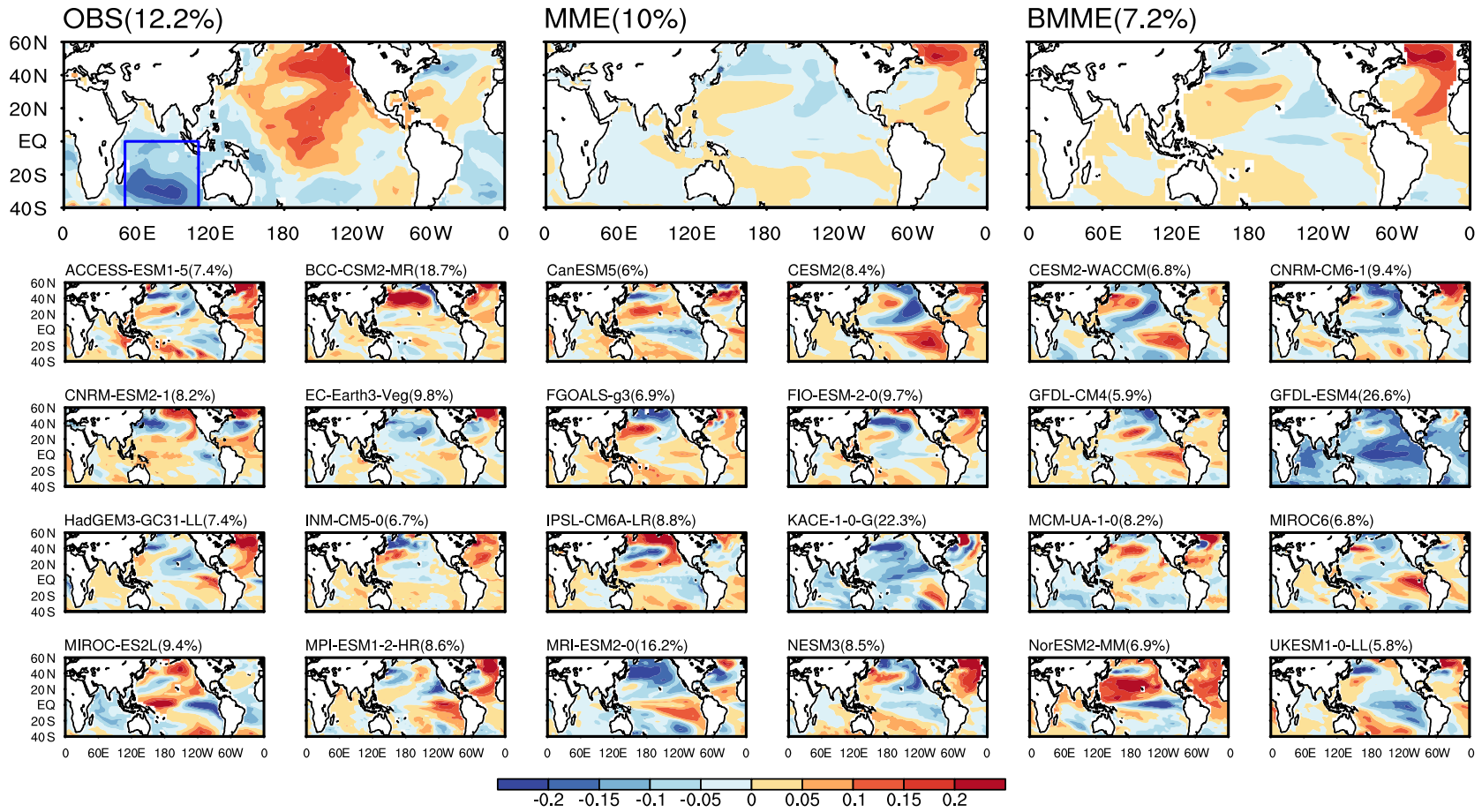

Supplementary Figure 5. The SIO mode in CMIP6 models' historical simulation and observation during the period of 1901-2014. The SIO mode of global SST in OBS, MME, BMME and individual models in historical run. The number on left conner of each subfigure represents the explained variance of the EOF mode. The result of MME (BMME) is the average of the SIO modes obtained from 24 CMIP6 models (best six models). The SIO domain is outlined by the blue lines in OBS.

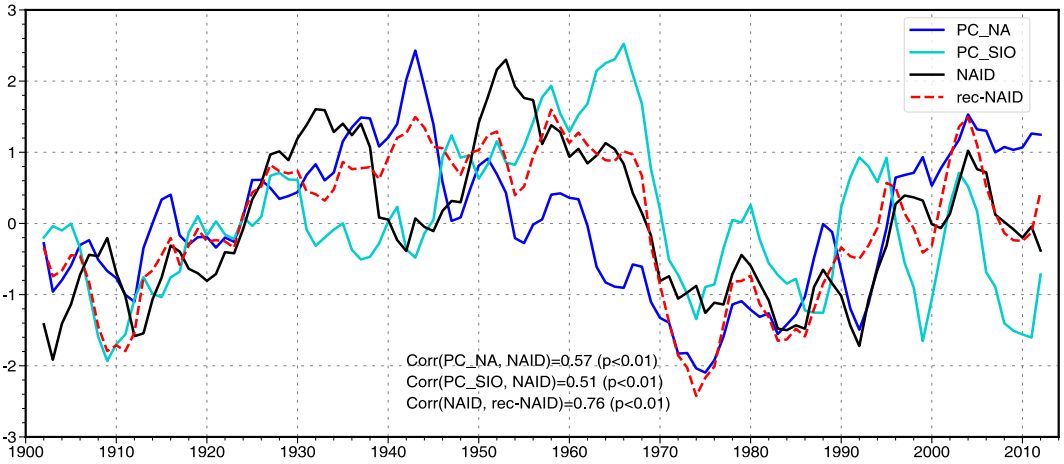

Supplementary Figure 6. The relationship between NAID index and the PC of NA (SIO) modes in observation during 1901-2014. The PC of NA (SIO) mode is denoted by blue line (indigo line). The observed NAID and reconstructed NAID index (rec-NAID) index is indicated by black line and red dash line, respectively. Th reconstructed NAID index is calculated as the equation: rec-NAID = 0.57×PC_NA + 0.51×PC_SIO.

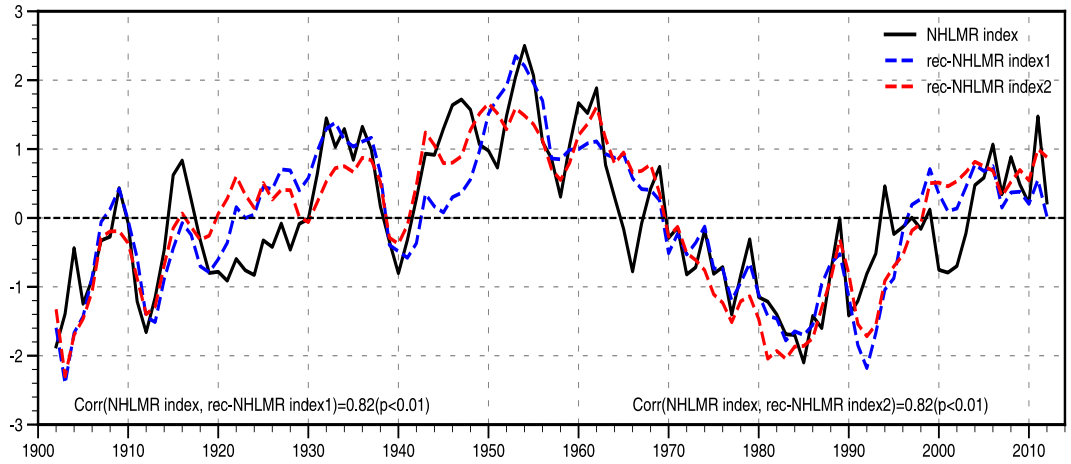

Supplementary Figure 7. The relationship between observed NHLMR index and reconstructed NHLMR indices during 1901-2014. The reconstructed NHLMR indices are computed using global SST anomaly modes. The first reconstructed NHLMR index, rec-NHLMR index1, is computed by the regression equation using observed EWPC and NAID as "predictors". Similarly, the rec-NHLMR index2 is computed by the regression equation using the PCs of the three major global SSTA modes (Methods).

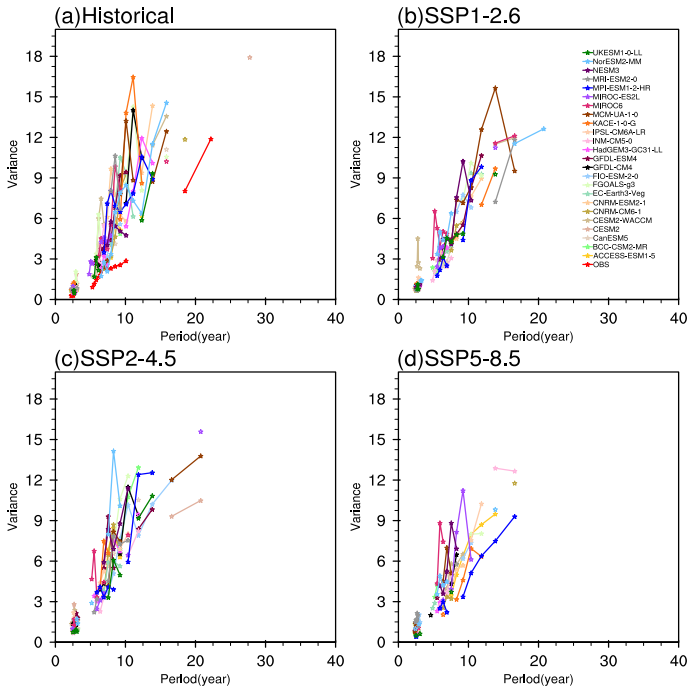

Supplementary Figure 8. Power spectra of decadal NHLMR index in observation and individual models. Spectra of decadal NHLMR index in (a) observation (red line) and historical simulations, as well as future projections under (b) SSP1-2.6, (c) SSP2-4.5 and (d) SSP5-8.5 scenarios. Only the significant periods ($p<0.1$) are shown. The period for the observation and historical simulations (future projections) is from 1901 to 2014 (2015 to 2100).

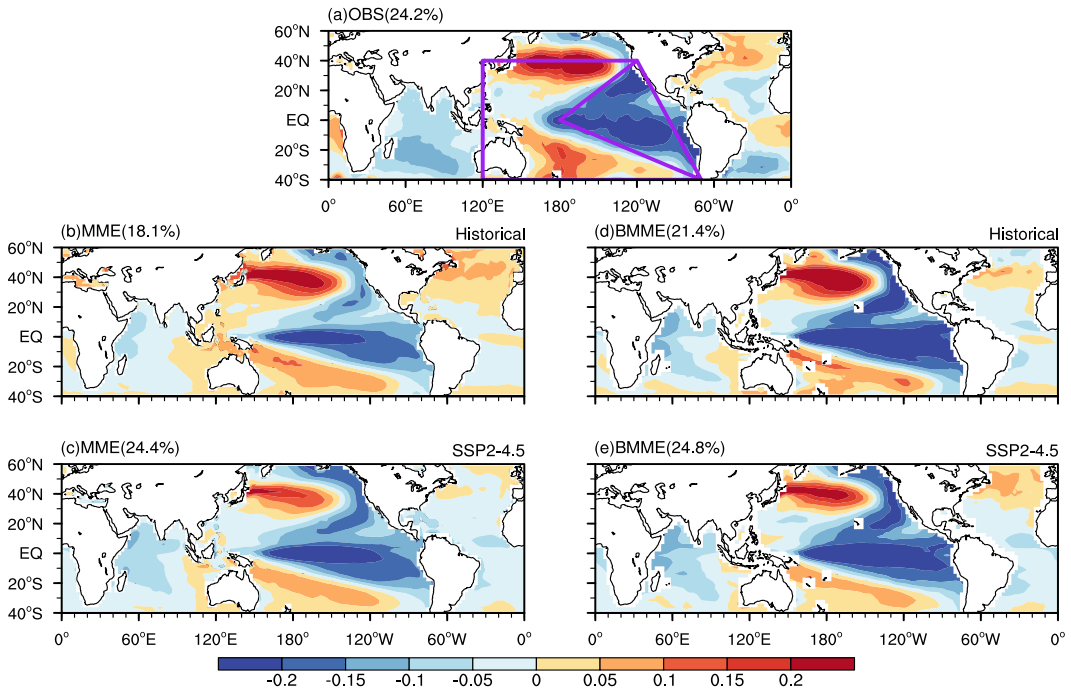

Supplementary Figure 9. The EWPC mode in observation and MME/BMME. The EWPC mode of global SST in (a) observation, and MME from (b) historical simulation as well as (c) future projection under SSP2-4.5 scenario. (d-e) are same as (b-c), but for BMME. The number on left corner of each subfigure represents the explained variance of the EOF mode. The result of MME (BMME) is the average of the EWPC modes obtained from all CMIP6 models. The EWPC domain is outlined by the purple lines in (a). The period for the observation and historical simulations (future projections) is from 1901 to 2014 (2015 to 2100).

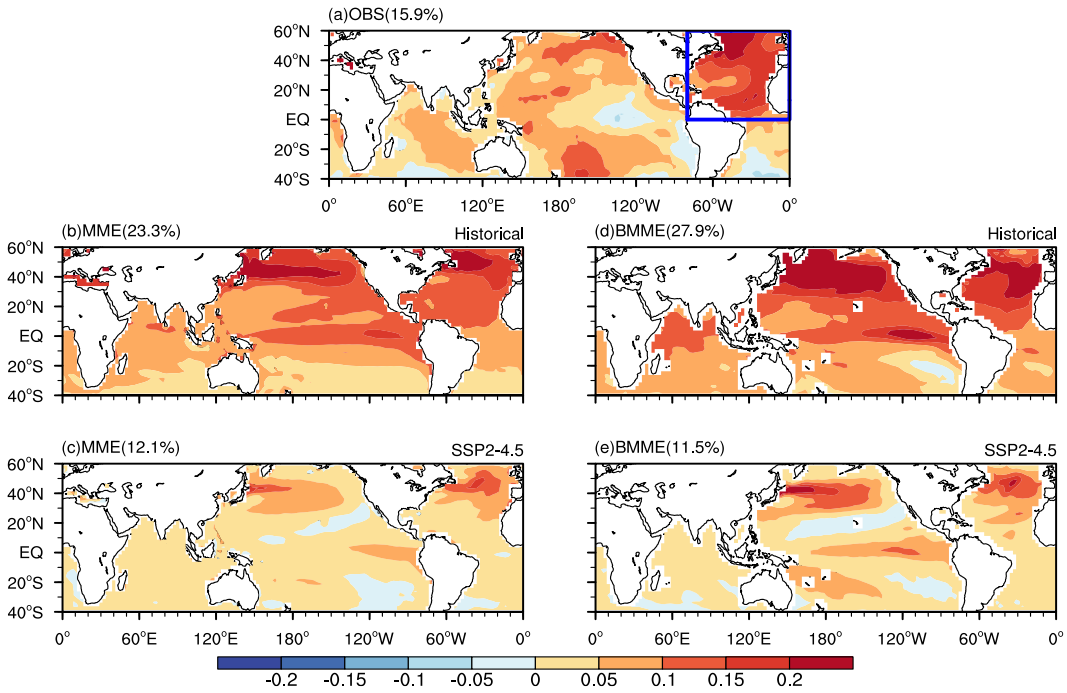

Supplementary Figure 10. The NA mode in observation and MME/BMME. The NA mode of global SST in (a) observation, and MME from (b) historical simulation as well as (c) future projection under SSP2-4.5 scenario. (d-e) are same as (b-c), but for BMME. The number on left corner of each subfigure represents the explained variance of the EOF mode. The result of MME (BMME) is the average of the NA modes obtained from all CMIP6 models. The NA domain is outlined by the blue lines in (a). The period for the observation and historical simulations (future projections) is from 1901 to 2014 (2015 to 2100).

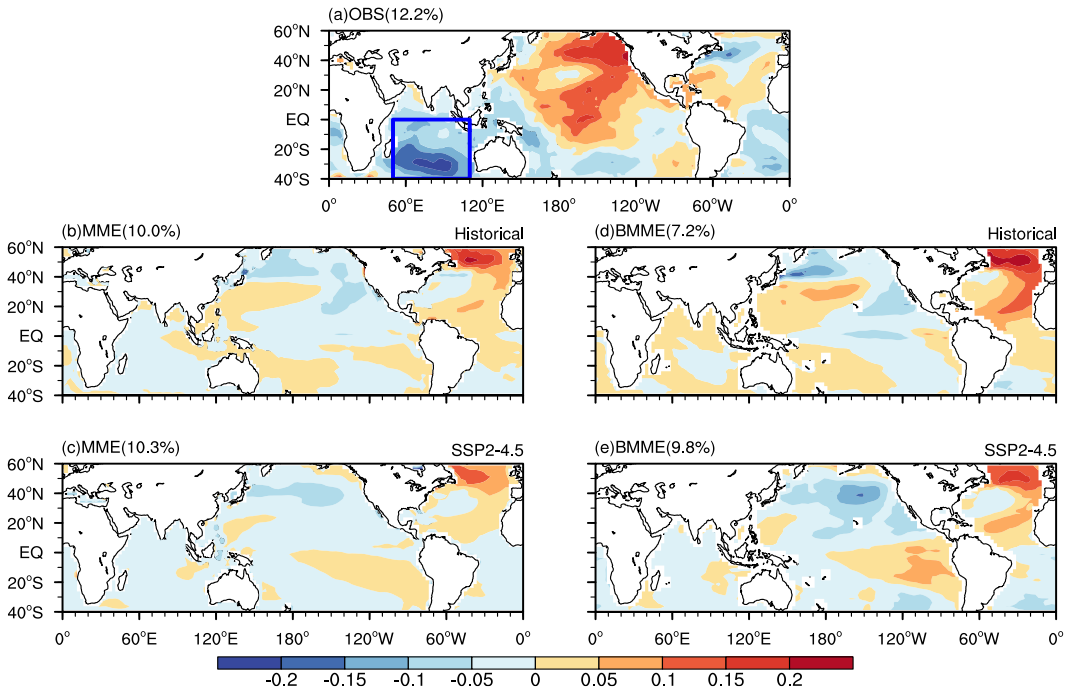

Supplementary Figure 11. The SIO mode in observation and MME/BMME. The SIO mode of global SST in (a) observation, and MME from (b) historical simulation as well as (c) future projection under SSP2-4.5 scenario. (d-e) are same as (b-c), but for BMME. The number on left corner of each subfigure represents the explained variance of the EOF mode. The result of MME (BMME) is the average of the SIO modes obtained from all CMIP6 models. The SIO domain is outlined by the blue lines in (a). The period for the observation and historical simulations (future projections) is from 1901 to 2014 (2015 to 2100).

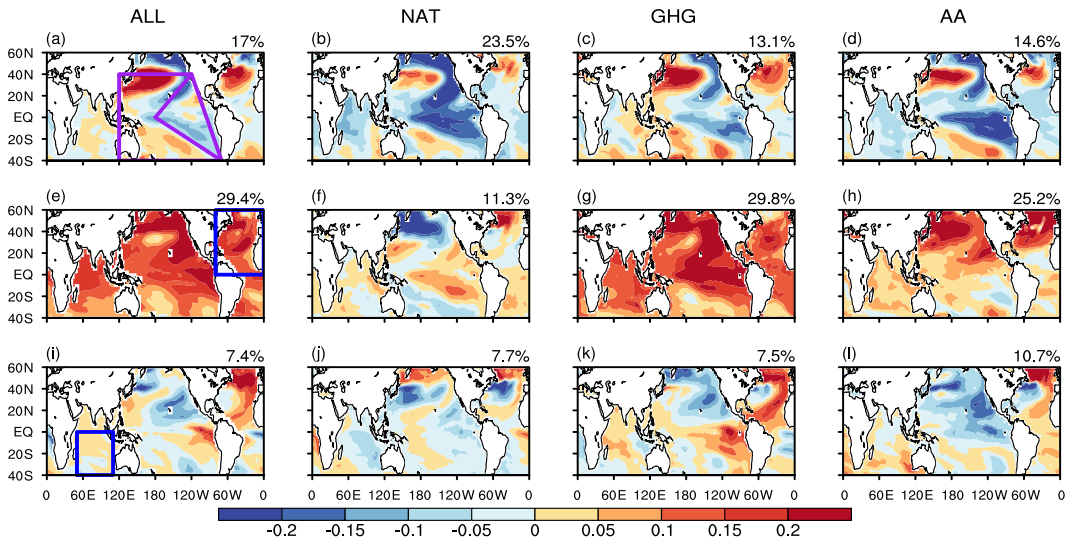

Supplementary Figure 12. The three major global SST modes under different forcings in HadGEM3-GC31-LL during historical period (1901-2014). The EWPC modes under (a) all forcing, the individual forcing of (b) natural forcing, (c) greenhouse gases and (d) anthropogenic aerosols simulations. (e-h), (i-l) are same as (a-d), but for the NA modes and SIO modes, respectively. The number in upper right indicates the explained variance of the EOF mode. The critical areas in EWPC, NA and SIO modes are outlined in (a) (e) (i) respectively.

Supplementary Table 1. The temporal correlation coefficient (TCC) between the NHLMR and PC1, EWPC, NAID obtained from MME and BMME in historical simulation (1901-2014), future projection under SSP2-4.5 scenario (2015-2100). The TCCs of MME (BMME) is the average of the temporal correlation coefficients obtained from all CMIP6 models (best six models). The bold TCCs are significant at a 95% confidence level.

	NHLMR&PC1		NHLMR&EWPC		NHLMR&NAID	
	hist	SSP2-4.5	hist	SSP2-4.5	hist	SSP2-4.5
MME	**0.58**	**0.49**	**0.56**	**0.48**	**0.35**	0.18
BMME	**0.85**	**0.56**	**0.62**	**0.57**	**0.50**	0.27

Supplementary Table 2. The TCCs between the global SST major modes and NHLMR-related oceanic drivers derived from observation, historical simulations (1901-2014), and future projections under SSP2-4.5 scenario (2015-2100). The columns from left to right represent the TCC between EWPC index and PC of EWPC mode, SIO index and PC of SIO mode, NA index and PC of NA mode, respectively. The TCCs of MME (BMME) is the average of the temporal correlation coefficients obtained from all CMIP6 models (best six models). The bold TCCs are significant at a 95% confidence level.

	EWPC&PC_EWPC		SIO&PC_SIO		NA&PC_NA	
OBS	**0.93**		**-0.74**		**0.92**	
	hist	SSP2-4.5	hist	SSP2-4.5	hist	SSP2-4.5
MME	**0.73**	**0.75**	-0.06	-0.17	**0.73**	**0.48**
BMME	**0.80**	**0.82**	0.04	-0.14	**0.76**	**0.52**

Supplementary Table 3. The impacts of external forcings on decadal NHLMR, and the relationships between global SST major modes and NHLMR-related oceanic drivers in historical run period (1901-2014). The TCC between NHLMR index and PC1 of NHLMR, and between PC of global SST major modes and the corresponding SSTA index conducted by all forcings (ALL), the individual forcing of natural forcing (hist-NAT), greenhouse gases (hist-GHG) and anthropogenic aerosol (hist-AA), respectively, in HadGEM3-GC31-LL. The bold TCCs are significant at a 95% confidence level.

	ALL	hist-NAT	hist-GHG	hist-AA
NHLMR index&PC1	**0.89**	**0.50**	**0.83**	**0.69**
PC_EWPC&EWPC index	**0.75**	**0.83**	**0.71**	**0.82**
PC_NA&NA index	**0.77**	**0.28**	**0.67**	**0.87**
PC_SIO&SIO index	0.03	**-0.49**	0.07	0.21

Supplementary Table 4. Information of 24 CMIP6 models. The symbol "√" represents the model is available in historical or ScenarioMIP simulations.

Model	Institute/Country	Historical	SSP1-2.6	SSP2-4.5	SSP5-8.5
ACCESS-ESM1-5	CSIRO/Australian	√	√	√	√
BCC-CSM2-MR	BCC /China	√	√	√	√
CanESM5	CCCma/Canada	√	√	√	√
CESM2	NCAR/USA	√		√	
CESM2-WACCM	NCAR/USA	√	√	√	√
CNRM-CM6-1	CNRMCERFACS/France	√	√	√	√
CNRM-ESM2-1	CNRMCERFACS/France	√	√	√	√
EC-Earth3-Veg	EC-Earth-Consortium/EU	√	√	√	√
FGOALS-g3	CAS/China	√	√	√	√
FIO-ESM-2-0	FIO-QLNM/China	√	√	√	√
GFDL-CM4	NOAA GFDL/USA	√		√	√
GFDL-ESM4	NOAA GFDL/USA	√	√	√	√
HadGEM3-GC31-LL	MOHC/UK	√	√	√	√
INM-CM5-0	INM/Russia	√	√	√	√
IPSL-CM6A-LR	IPSL/France	√	√	√	√
KACE-1-0-G	NIMS-KMA/Korea	√	√	√	√
MCM-UA-1-0	UA/USA	√	√	√	√
MIROC6	MIROC/Japan	√	√	√	√
MIROC-ES2L	MIROC/Japan	√	√	√	√
MPI-ESM1-2-HR	MPI-M/Germany	√	√	√	√
MRI-ESM2-0	MRI/Japan	√	√	√	√
NESM3	NUIST/China	√	√	√	√
NorESM2-MM	NCC/Norway	√	√	√	√
UKESM1-0-LL	MOHC/UK	√	√	√	√